ChemComm

Accepted Manuscript

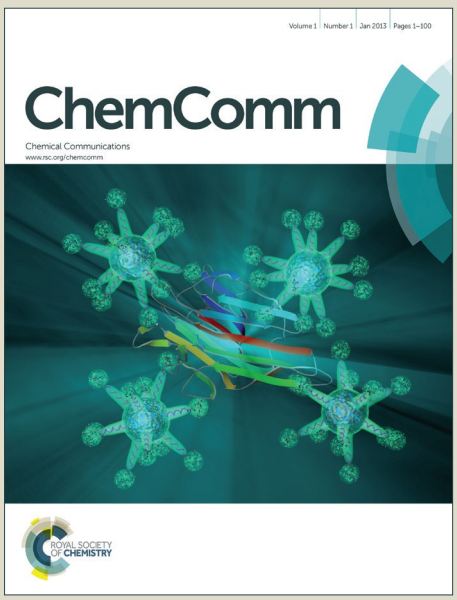

This is an *Accepted Manuscript*, which has been through the Royal Society of Chemistry peer review process and has been accepted for publication.

Accepted Manuscripts are published online shortly after acceptance, before technical editing, formatting and proof reading. Using this free service, authors can make their results available to the community, in citable form, before we publish the edited article. We will replace this *Accepted Manuscript* with the edited and formatted *Advance Article* as soon as it is available.

You can find more information about *Accepted Manuscripts* in the Information for Authors.

Please note that technical editing may introduce minor changes to the text and/or graphics, which may alter content. The journal's standard Terms & Conditions and the Ethical guidelines still apply. In no event shall the Royal Society of Chemistry be held responsible for any errors or omissions in this *Accepted Manuscript* or any consequences arising from the use of any information it contains.

ROYAL SOCIETY OF CHEMISTRY

www.rsc.org/chemcomm

Please do not adjust margins

Journal Name

COMMUNICATION

Low-temperature fabrication of brown TiO_2 with enhanced photocatalytic activities under visible light

Received 00th January 20xx,
Accepted 00th January 20xx

DOI: 10.1039/x0xx00000x

www.rsc.org/

Mingzheng Wang,[a,b,#] Biao Nie,[b,#] Ka-Kit Yee,[c] Haidong Bian,[b,c] Chris Lee,[b] Hung Kay Lee,[d] Bo Zheng,[d] Jian Lu,[e,f] Linbao Luo,[a] Yang Yang Li [b,g,*]

Here we report a facile one-step low-temperature solution-based method to treat native TiO_2 with NaH. The NaH treatment effectively induces the Ti(III) species and oxygen vacancies into the TiO_2 host lattice, and enables the absorption edge of TiO_2 to be conveniently adjusted from the UV region to the red end of the visible spectrum.

Titanium oxide (TiO_2), as a type of widely studied photocatalyst, offers attractive technological advantages, but presents outstanding limitations at the same time. The former includes high stability, low toxicity and wide commercial availability—advantages that are crucial for large-scale applications in energy and environment areas (e.g., electrode material, hydrogen production and water decontamination).[1] Native forms of TiO_2, however, have a wide electronic bandgap (e.g., 3.0 and 3.2 eV for rutile and anatase); as a result, only UV or higher-energy photons can be effectively absorbed by native TiO_2, while the visible light and longer-wavelength photons cannot. As UV light only covers a small fraction (3-5%) of the solar spectrum (the visible/infrared region is dominant), TiO_2 in the native forms is generally not efficient in harnessing solar energy for photocatalytic applications.

Intensive efforts are therefore being made to modify the absorption behaviours of TiO_2, in order to achieve higher responsiveness to the abundant visible light in the solar spectrum. Several strategies have been reported. One common strategy is to mix in additives or reductants with the titanium compound precursors in the preparative process so that the resultant TiO_2 is doped with $Ti3^+$ or other impurity centers.[2] This can be accomplished using various approaches, e.g., the sol-gel[2b, 2f, 3] or hydrothermal methods.[4] Another modification approach that is being intensively investigated is to directly modify native TiO_2. This is usually done by heating native TiO_2 in a particular atmosphere (e.g., H_2, NH_3 or N_2).[5] By means of thermal treatments, TiO_2 products doped with various impurity atoms (e.g., N),[5e] self-doped with Ti^{3+} centers[5a] have been successfully made. Among these, H_2-thermal treatment[5a-d, 6] has lately attracted much attention as a particularly effective method to generate TiO_2 with broader light absorption and outstanding photocatalytic properties in solar or visible light. Mechanisms accounting for absorption edge extension have been suggested to involve the emergence of the Ti^{3+} ions or oxygen vacancies in the H_2-treated TiO_2 samples.[5a, 5c, 5d, 6a] In addition, a recent breakthrough reported by Chen et al.[5b, 5c] pointed to a novel modification mechanism: through the introduction of surface disorders.[5b, 5c, 6a, 7] In spite of these encouraging progress achieved, the reported hydrogenation procedures generally involve high safety risk due to the application of high-temperature (e.g., 500 °C) or high-pressure (e.g., 20 bar) H_2.

Here we report a facile solution-based method (the experimental details are shown in ESI) to modify native TiO_2 via treatment with a NaH solution under the mild condition of low temperature (e.g., 150 °C) and atmospheric pressure, thus lowering the safety hazard associated with the reported

[a] School of Electronic Science and Applied Physics, Hefei University of Technology, Hefei, Anhui 230009, China.

[b] Center Of Super-Diamond and Advanced Films (COSDAF), Centre for Functional Photonics, and Department of Physics and Materials Science, City University of Hong Kong, Kowloon, Hong Kong.

[c] Department of Biology and Chemistry, City University of Hong Kong, Kowloon, Hong Kong.

[d] Department of Chemistry, Chinese University of Hong Kong, Shatin, Hong Kong.

[e] Department of Mechanical and Biomedical Engineering, and Center for Advanced Structural Materials, City University of Hong Kong, Kowloon, Hong Kong.

[f] Centre for Advanced Structural Materials, City University of Hong Kong Shenzhen Research Institute, 8 Yuexing 1st Road, Shenzhen Hi-Tech Industrial Park, Nanshan District, Shenzhen, China.

[g] City University of Hong Kong Shenzhen Research Institute, 8 Yuexing 1st Road, Shenzhen Hi-Tech Industrial Park, Nanshan District, Shenzhen, China. Tel: 852-3442-7810; E-mail: yangli@cityu.edu.hk

[#] Equally contributing authors

Electronic Supplementary Information (ESI) available: [details of any supplementary information available should be included here]. See DOI: 10.1039/x0xx00000x

ChemComm Accepted Manuscript

Please do not adjust margins

hydrogenation methods that entail high-temperature/pressure H_2. Using this solution protocol, doped TiO_2 solid samples featuring adjustable absorption edges (from UV to the red light[8]) and largely enhanced photo-activities in visible light, can be conveniently prepared. In particular, brown-colored (**Fig. 1, Fig. S1**) TiO_2 solids can be fabricated, adding another hue to the color selection[2e, 5b, 5c, 6a, 9] of modified TiO_2 products.

Distinct color change from white to brown was readily observed in the above treatment of TiO_2 by NaH (i.e., Sample D; see Fig. 1). The TEM study (**Fig. 2**a-c) revealed that the particle sizes of native (P-25) and treated (sample D, shown in Table S1) TiO_2 particles were in the range of 20 ~ 50 nm, whereas the elemental analysis of both samples by EDS (**Fig. 2**c) suggested a chemical formula consistent with TiO_2 (i.e., the degree of doping was not detectable by EDS).

The commercial native TiO_2 nanoparticles (P-25) possess mixed crystal phases of anatase and rutile with a weight ratio of approximately 4/1. The XRD patterns (**Fig. 2**d) of P-25 and NaH-treated TiO_2 (Samples A-D) indicated that the crystallinity of the TiO_2 solid was maintained before and after the treatment, with no impurity peaks observed. However, the diffraction peaks of Samples A-D shifted to the larger diffraction angles comparing to P-25 (the shift was particularly more apparent for the higher-order peaks), indicating a smaller lattice spacing in the NaH-treated samples. Furthermore, lower peak intensities were observed on the treated TiO_2 (particularly Sample D), suggesting an increased level of defects resulted from the treatment. This observation is in good agreement with the TiO_2 samples doped using other methods.[5b]

To investigate the chemical environment and states of Ti and O in the treated TiO_2, XPS measurements were performed. The XPS spectra of native TiO_2 (P-25) (**Fig. 3**a) and treated (Sample D) TiO_2 (**Fig. 3**b) indicated that Ti, O elements and a trace amount of C and Na were present in the samples. The high-resolution Ti2p spectra (**Fig. 3**c) indicated an apparent shift towards the lower energy end for the peaks of NaH-treated TiO_2 (457.2 eV), relative to native TiO_2 (458.6 eV). This observation is thus in line with the presence of Ti^{3+} in the NaH-treated TiO_2 samples, for the major Ti2p peak for Ti^{3+} is normally found at lower energy (around 457.7 eV) than that of Ti^{4+} (459.5 eV).[5a] Moreover, the XPS study also suggested the formation of oxygen vacancies resulted from the NaH treatment. The O1s spectra (**Fig. 3**d) distinctly showed a new peak emerging at 531.2 eV, which can be ascribed to the existence of oxygen-vacancy sites nearby Ti^{3+}.[2e, 7] One weak peak located at 1072.7 eV corresponding to the Na1s core levels was observed in the high-resolution Na1s spectrum (inset of **Fig. 3**b), indicating the presence of Na^+ in the treated TiO_2 samples.

The UV-Vis diffuse reflectance spectra (**Fig. 4**a) showed that, comparing to native TiO_2, the absorption edges of NaH-treated TiO_2 shifted to longer wavelengths in the visible region. The spectrum of native TiO_2 showed a single steep absorption edge around 400 nm corresponding to its bandgap. Clearly, NaH-treated TiO_2 exhibited different optical responses (**Fig. 4**a, **Fig. S2**). In particular, Sample D displayed considerable absorption in the visible region between 400 and 700 nm, consistent with its brown-colored appearance.

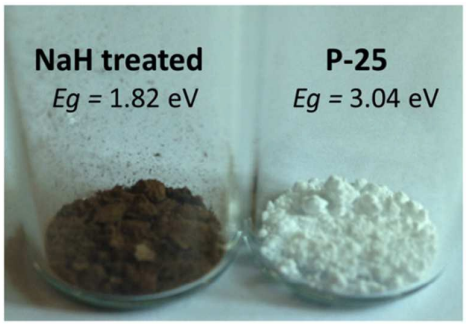

Fig. 1 Photographs of commercial (P-25) and NaH-treated (Sample D) TiO_2.

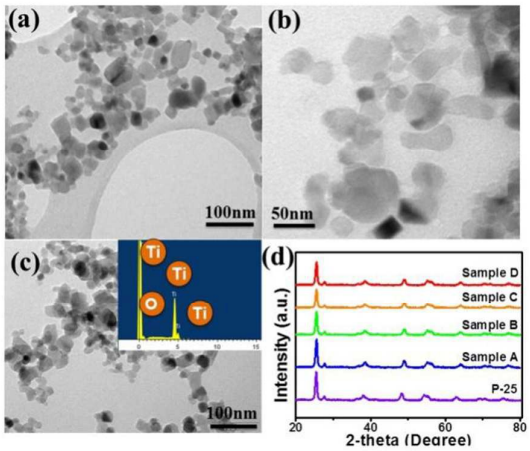

Fig. 2 TEM images of commercial (a) and NaH-treated TiO_2 nanoparticles (b) (c) and the inset shows the EDS spectrum of NaH-treated TiO_2. (d) XRD patterns of commercial TiO_2 (P-25) and Samples A-D whose fabrication conditions were shown in Table S1.

The Kubelka-Munk function, F(R), as a function wavelength was derived from the measured diffuse reflectance spectra, based on the Kubelka-Munk equation:[10]

$$F(R) = \frac{(1-R)^2}{2R}$$

where R is the ratio of the sample reflectance to the reference reflectance. A Tauc plot $([F(R) \cdot h\nu]^{1/2}$ vs. hv, where hv is the photon energy) was then obtained (**Fig. 4**b). The absorption edge was determined from the extrapolation of the linear fit for the Tauc plot onto the energy axis. Note that the Tauc plot is commonly used for determining the absorption edge of TiO_2 in literature.[11] It was estimated that absorption edge is 3.04 eV for native TiO_2 and 2.69, 2.32, 2.11 and 1.82 eV for Samples A-D, respectively (Table S1). Previous studies show that, as the concentration of the Ti^{3+} ions/oxygen vacancies increase, the band tailing becomes more evident and lowered absorption edge is resulted.[5a, 6a] The gradual lowering of the absorption edge from Samples A to D indicates the gradual increasing concentration of the Ti^{3+} ions/oxygen vacancies in these samples. The finding that P-25 (native TiO_2) showed a lower absorption edge than the bulk anatase (Eg = 3.2 eV) is in good agreement with previous studies, and can be ascribed to the fact that that P-25 is mix-phased nanoparticles containing ~ 25% rutile phase and 75% anatase phase.[2f]

A possible reaction mechanism leading to the formation of the Ti^{3+} ions and the oxygen vacancies by the NaH treatment are shown in eqs. 1-3. First, the H^- ions supplied by NaH bond

ChemComm Accepted Manuscript

 This journal is © The Royal Society of Chemistry 20xx

with Ti^{4+} to form a titanium hydride species $[TiH]^{3+}$; the $[TiH]^{3+}$ species then disintegrate to give the Ti^{3+} centers and H· radicals that readily combine to form H_2 gas. The charge balance is likely maintained by intercalation of Na^+ ions into the host lattice of TiO_2, generating confined defects featuring local stoichiometry of $NaTiO_2$.

$$Ti^{4+} + H^- \rightarrow [Ti\text{-}H]^{3+} \quad (1)$$

$$[Ti\text{-}H]^{3+} \rightarrow Ti^{3+} + \bullet H \quad (2)$$

$$2 \bullet H \rightarrow H_2\uparrow \quad (3)$$

A comparison between Samples A and D (0.9 eV difference in absorption edge) indicates that the UV irradiation applied during the NaH treatment can result in a markedly lower absorption edge in the treated TiO_2 product. Previous studies has shown that trace amount of the Ti(III) species can be produced transiently in irradiated TiO_2.[12] The significant impact of UV irradiation observed here could be attributed to the UV-photon generated electrons and holes in TiO_2. The photogenerated electron-hole pairs may facilitate the doping process (see eqs. 4-6), e.g., the positive holes generated in the valence band of TiO_2 is highly oxidizing, and therefore more readily accepts electrons from the H^- ions compared with the TiO_2 system without excitation by UV light. Furthermore, because the electron-hole pairs can be UV-excited not only at the surface layer but also inside the TiO_2 lattice, Ti^{3+} can be produced (eq. 5) deeper inside the TiO_2 lattice. Comparing to those on the surface, the Ti^{3+} ions inside the TiO_2 are likely much less susceptible to oxidation by oxygen,[9] leading to a higher stability of the treated TiO_2 when placed in the ambient environment.

$$TiO_2 + h\nu \rightarrow TiO_2 + e^-_{CB} + h^+_{VB} \quad (4)$$

$$Ti^{4+} + e^-_{CB} \rightarrow Ti^{3+} \quad (5)$$

$$h^+_{VB} + H^- \rightarrow \bullet H \quad (6)$$

Comparison between Samples B and D shows that a higher reaction temperature (e.g., by 30 °C) can lead to a substantial reduction of the absorption edge (e.g., by ~0.5 eV). In general, the reductive doping of the very stable TiO_2 solid is a slow process. The great effects of higher temperature and UV treatment in lowering the absorption edge of the doped TiO_2 product help to highlight the underlying reasons for the success of the current strategy for self-doping TiO_2.

To examine the presence and distribution of Ti(III) in the samples, the ESR measurements were carried out. No signal due to the paramagnetic Ti(III) species were observed in the NaH-treated samples (**Fig. S3**). This can be possibly due to the formation of a di-Ti(III) species, in which the two Ti(III) centers anti-ferromagnetically couple with each other forming a diamagnetic binuclear compound that is EPR silent. For Sample A, a weak signal occurring around 1600 Gauss was observed, which can be attributed to some residual Fe(III) impurities introduced to the system during the sample handling (e.g., from the steel spatula).

Compared with native TiO_2, the NaH-treated TiO_2 samples all displayed higher ability to photo-degrade phenol, with the degradation rates gradually increasing from Sample A to Sample D (**Fig. 4**). It is noted that no significant adsorption of the organic molecules onto the samples was observed in darkness (**Fig. S4**). To explain the higher photo-degradation rate observed on NaH-treated TiO_2, a discussion on the photo-degradation mechanism is helpful. TiO_2 is an n-type semiconductor. For native TiO_2, when illuminated with UV photons with energy higher than its bandgap, the photo-excited electrons in the conduction band (CB) can be transferred to the O_2 molecules absorbed on the surface of TiO_2 and form oxygen radicals, $\bullet O_2^-$, that can degrade the absorbed organic molecules. For treated TiO_2, previous studies indicate that the Ti^{3+} ions/oxygen vacancies induce donor levels in the bandgap (a higher concentration of the Ti^{3+} ions/oxygen vacancies leads to more donor levels in the band gap).**Error! Bookmark not defined.**[,Error! Bookmark not defined.] These donor levels may help trap the photogenerated electrons which generate $\bullet O_2^-$, lessening the recombination of the photogenerated electrons and holes. Therefore, under UV irradiation, the existence of the donor states bestows upon NaH-treated TiO_2 enhanced photocatalytic activity, with the wider tail band leading to the greater enhancement.

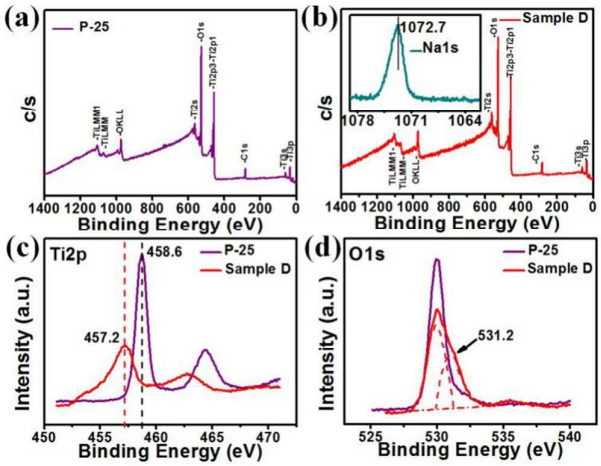

Fig. 3 XPS spectra of commercial TiO_2 (P-25) (a) and Sample D (b) with the high-resolution Na1s spectrum of Sample D shown in the inset in (b). The high-solution Ti2p and O1s XPS spectra of commercial TiO_2 (P-25) and Sample D are shown in (c) and (d), respectively.

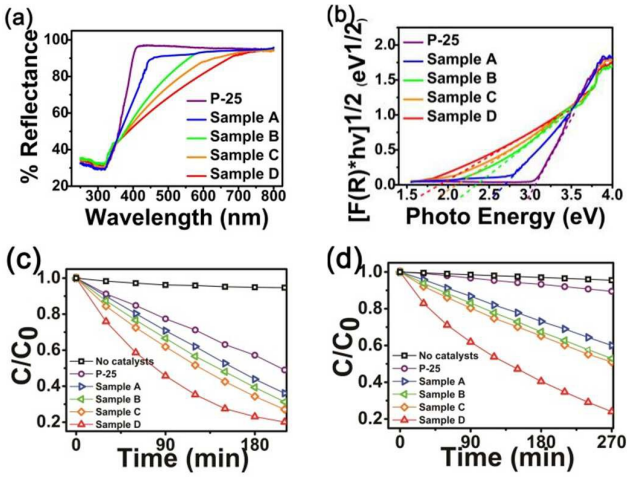

Fig. 4 Reflectlance spectra (a) and Tauc plots (b) of commercial TiO_2 (P-25) and Samples A-D. Photodegradation rate of phenol under UV (c) and visible (d) illumination, measured with commercial TiO_2 (P-25) and Samples A-D.

ChemComm Accepted Manuscript

Notably, the enhancement effect on photodegradation under UV irradiation is not as dramatic as under visible illumination (**Fig. 4**c-d). This is because the photon energies of visible light are insufficient to excite native TiO_2 but high enough to excite NaH-treated TiO_2. It was found that TiO_2 with a lower absorption edge displayed higher photodegrading efficiency, possibly because they utilized a larger portion of the visible spectrum and possessed more donor levels to trap more photo-excited electrons which in turn generate more $\bullet O_2^-$. A closer look at **Fig. 4**d reveals that, under visible irradiation, the degradation rate for native TiO_2 is very low but slightly higher than when no catalyst was used. It is well known that native TiO_2 cannot be excited by visible light because of its wide bandgap. This observed slight photodegradation ability of native TiO_2 under the visible light irradiation is possibly caused by the photo-sensitizing capability of the dye molecules which can be excited by the visible light and inject electrons to the conduction band of TiO_2.[1e]

The NaH-treated TiO_2 samples did not change color after stored in dark in air at room temperature for 6 months. The photocatalytic properties and the performance stability (**Fig. S5**) of the NaH-treated TiO_2 can be potentially further improved by increasing the temperature, time, and UV light intensity used for the NaH treatment. In the second photodegradation test, NaH-treated TiO_2 showed reduced activity, although still better than P-25. This activity reduction observed is possibly due to the decreased concentrations of Ti^{3+} and the oxygen vacancies in the samples. Oxygen vacancies and Ti^{3+} are not very stable and can be susceptible to oxidation by the dissolved oxygen molecules in solution.[13]

In summary, brown-color TiO_2 with the absorption edge in red light has been conveniently fabricated using a facile one-step treatment in a NaH solution. The dramatic absorption edge lowering is attributed to the Ti^{3+} ions/oxygen vacancies created by the NaH treatment. The fabricated brown TiO_2 showed significantly higher photocatalytic activity than untreated commercial TiO_2. The outstanding photocatalytic performance and the great fabrication convenience enabled by the novel method presented in this study open a new route to practical applications of TiO_2 under visible light. Besides photodegradation of organic molecules presented here, the NaH-treated TiO_2 is potentially promising for solar water splitting applications as well. Furthermore, the method reported here can be potentially applied for modifying other metal oxide semiconductor systems, based on the fact that metal oxide semiconductors generally share similar modification mechanisms.

This work was supported by the National Key Basic Research Program of the Chinese Ministry of Science and Technology (Grant 2012CB932203), the National Natural Science Foundation of China (Project 51202206), and the Hong Kong Research Grants Council (RGC) General Research Funds (GRF) (Grant No. CityU 11302515).

Notes and references

1 (a) A. Fujishima, *Nature*, 1972, **238**, 37-38; (b) L. Yu, Z. Wang, L. Zhang, H. B. Wu and X. W. D. Lou, *J. Mater. Chem. A*, 2013, **1**, 122-127; (c) O. Carp, C. L. Huisman and A. Reller, *Prog. Solid State Chem.*, 2004, **32**, 33-177; (d) J. SongáChen, Y. LingáCheah and X. WenáLou, *J. Mater. Chem.*, 2011, **21**, 1677-1680; (e) X. Chen and S. S. Mao, *Chem. Rev.*, 2007, **107**, 2891-2959.

2 (a) B. Liu, L.-M. Liu, X.-F. Lang, H.-Y. Wang, X. W. Lou and E. S. Aydil, *Energy Environ. Sci.*, 2014, **7**, 2592-2597; (b) J. C. Yu, J. Yu, W. Ho, Z. Jiang and L. Zhang, *Chem. Mater.*, 2002, **14**, 3808-3816; (c) F. Zuo, L. Wang, T. Wu, Z. Zhang, D. Borchardt and P. Feng, *J. Am. Chem. Soc.*, 2010, **132**, 11856-11857; (d) T. Ohno, M. Akiyoshi, T. Umebayashi, K. Asai, T. Mitsui and M. Matsumura, *Appl. Catal., A*, 2004, **265**, 115-121; (e) Z. Zheng, B. Huang, X. Meng, J. Wang, S. Wang, Z. Lou, Z. Wang, X. Qin, X. Zhang and Y. Dai, *Chem. Commun.*, 2013, **49**, 868-870; (f) W. Choi, A. Termin and M. Hoffmann, *J. Phys. Chem*, 1994, 13669-13679; (g) S. Klosek and D. Raftery, *J. Phys. Chem. B*, 2001, **105**, 2815-2819; (h) X. Chen and C. Burda, *J. Am. Chem. Soc.*, 2008, **130**, 5018-5019; (i) S.-T. Myung, M. Kikuchi, C. S. Yoon, H. Yashiro, S.-J. Kim, Y.-K. Sun and B. Scrosati, *Energy Environ. Sci.*, 2013, **6**, 2609-2614.

3 (a) C. Burda, Y. Lou, X. Chen, A. C. Samia, J. Stout and J. L. Gole, *Nano Lett.*, 2003, **3**, 1049-1051; (b) Q. Xiao, J. Zhang, C. Xiao, Z. Si and X. Tan, *Sol. Energy*, 2008, **82**, 706-713; (c) E. Wang, W. Yang and Y. Cao, *J. Phys. Chem. C*, 2009, **113**, 20912-20917; (d) A. T. Kuvarega, R. W. M. Krause and B. B. Mamba, *J. Phys. Chem. C*, 2011, **115**, 22110-22120.

4 (a) H. G. Yang, G. Liu, S. Z. Qiao, C. H. Sun, Y. G. Jin, S. C. Smith, J. Zou, H. M. Cheng and G. Q. Lu, *J. Am. Chem. Soc.*, 2009, **131**, 4078-4083; (b) G. Liu, H. G. Yang, X. Wang, L. Cheng, J. Pan, G. Q. Lu and H.-M. Cheng, *J. Am. Chem. Soc.*, 2009, **131**, 12868-12869.

5 (a) X. Lu, G. Wang, T. Zhai, M. Yu, J. Gan, Y. Tong and Y. Li, *Nano Lett.*, 2012, **12**, 1690-1696; (b) X. Chen, L. Liu, Y. Y. Peter and S. S. Mao, *Science*, 2011, **331**, 746-750; (c) X. Chen, L. Liu, Z. Liu, M. A. Marcus, W.-C. Wang, N. A. Oyler, M. E. Grass, B. Mao, P.-A. Glans and Y. Y. Peter, *Scientific Reports*, 2013, **3**, 1510; (d) G. Wang, Y. Ling and Y. Li, *Nanoscale*, 2012, **4**, 6682-6691; (e) H. Irie, Y. Watanabe and K. Hashimoto, *J. Phys. Chem. B*, 2003, **107**, 5483-5486; (f) R. Asahi, T. Morikawa, T. Ohwaki, K. Aoki and Y. Taga, *Science*, 2001, **293**, 269-271.

6 (a) G. Wang, H. Wang, Y. Ling, Y. Tang, X. Yang, R. C. Fitzmorris, C. Wang, J. Z. Zhang and Y. Li, *Nano Lett.*, 2011, **11**, 3026-3033; (b) A. Naldoni, M. Allieta, S. Santangelo, M. Marelli, F. Fabbri, S. Cappelli, C. L. Bianchi, R. Psaro and V. Dal Santo, *J. Am. Chem. Soc.*, 2012, **134**, 7600-7603.

7 T. Leshuk, R. Parviz, P. Everett, H. Krishnakumar, R. A. Varin and F. Gu, *ACS Appl. Mat. Interfaces*, 2013, **5**, 1892-1895.

8 (a) G. Liu, L. Wang, C. Sun, X. Yan, X. Wang, Z. Chen, S. C. Smith, H.-M. Cheng and G. Q. Lu, *Chem. Mater.*, 2009, **21**, 1266-1274; (b) G. Liu, L.-C. Yin, J. Wang, P. Niu, C. Zhen, Y. Xie and H.-M. Cheng, *Energy Environ. Sci.*, 2012, **5**, 9603-9610.

9 T. R. Gordon, M. Cargnello, T. Paik, F. Mangolini, R. T. Weber, P. Fornasiero and C. B. Murray, *J. Am. Chem. Soc.*, 2012, **134**, 6751-6761.

10 J. Tauc, *Mater. Res. Bull.*, 1970, **5**, 721-729.

11 (a) K. Madhusudan Reddy, S. V. Manorama and A. Ramachandra Reddy, *Mater. Chem. Phys.*, 2003, **78**, 239-245; (b) G. K. Mor, O. K. Varghese, M. Paulose and C. A. Grimes, *Adv. Funct. Mater.*, 2005, **15**, 1291-1296; (c) S. K. Mohapatra, M. Misra, V. K. Mahajan and K. S. Raja, *J. Phys. Chem. C*, 2007, **111**, 8677-8685.

12 (a) A. Henglein, *Chem. Rev.*, 1989, **89**, 1861-1873; (b) G. Rothenberger, J. Moser, M. Graetzel, N. Serpone and D. K. Sharma, *J. Am. Chem. Soc.*, 1985, **107**, 8054-8059.

13 (a) X. Pan, M.-Q. Yang, X. Fu, N. Zhang and Y.-J. Xu, *Nanoscale*, 2013, **5**, 3601-3614; (b) X. Jiang, Y. Zhang, J. Jiang, Y. Rong, Y. Wang, Y. Wu and C. Pan, *J. Phys. Chem. C*, 2012, **116**, 22619-22624.

ChemComm Accepted Manuscript

This journal is © The Royal Society of Chemistry 20xx